High-resolution IC inspection technique

Stephen Bradley Ippolito*, Anna K. Swan, Bennett B. Goldberg, and M. Selim Ünlü, Department of Electrical and Computer Engineering and the Photonics Center, Boston University, 8 Saint Mary's Street, Boston, Massachusetts 02215

We demonstrate a through the substrate, numerical aperture increasing lens (NAIL) technique for high-resolution inspection of silicon devices. We experimentally demonstrate a resolution of 0.2 μm, with the ultimate diffraction limit of 0.14 μm. Absorption limits inspection in silicon to wavelengths greater than 1 μm, placing an ultimate limit of 0.5 μm resolution on standard subsurface microscopy techniques. Our numerical aperture increasing lens reduces this limit to 0.14 μm, a significant improvement for device visual inspection (patent pending). The NAIL technique yields a resolution improvement over standard optical microscopy of at least a factor of n, the refractive index of the substrate material, and up to a factor of n^2. In silicon, this constitutes a resolution improvement between 3.6 and 13. This is accomplished by increasing the numerical aperture of the imaging system, without introducing any spherical aberration to the collected light. A specialized lens made of the same material as the substrate is placed on the back surface of the substrate. The convex surface of this lens is spherical with a radius of curvature, R. The vertical thickness of the lens, D, should be selected according to D = R (1+1/n)-X and the substrate thickness X.

Keywords: visual inspection silicon numerical aperture diffraction limited through substrate imaging

The lateral spatial resolution of standard optical microscopy is limited by diffraction to about half the wavelength of light. In surface microscopy reducing the wavelength or increasing the collected solid angle can improve the resolution. Oil immersion and solid immersion lens microscopy techniques reduce the wavelength by immersing the object space in a material with a higher refractive index. However, in subsurface microscopy the only way to improve the resolution is to increase the collected solid angle.

In accordance with the Sparrow criterion[1] most standard beam profiles have a spatial resolution limit near $\lambda_0/(2\times NA)$ where λ_0 is the free space wavelength of light. Therefore, to improve the resolution limit, the numerical aperture (*NA*) must be increased. The definition of *NA* is $n\times\sin\theta$ where *n* is the refractive index in the object space and θ is the half-angle of collection.

* ippolito@bu.edu

A standard microscope objective lens in air ambient shown in Fig. 1(a) will always have *NA* less than 1, with a typical best value of 0.95. By immersing the object space in a material with a higher refractive index (*n*) the *NA* can be improved. In Fig. 1(b) oil is inserted between a special oil immersion microscope objective lens and a sample. This oil immersion technique allows for *NA* values up to 1.4. A microscope design utilizing a high refractive index hemispherical lens, called a solid immersion lens (SIL)[2] is shown in Fig. 1(c). This technique relies on the evanescent coupling between the light focused at the geometrical center of the SIL spherical surface and closely spaced sample. The truncated sphere super-SIL of Fig. 1(d) not only increases *n*, but also increases θ by refraction at the spherical surface[3,4]. The solid immersion lens techniques yield the highest *NA* values in surface microscopy, using a GaP SIL a *NA* of 2 has been demonstrated[5]. By increasing *n*, these techniques have significantly improved the resolution of surface microscopy.

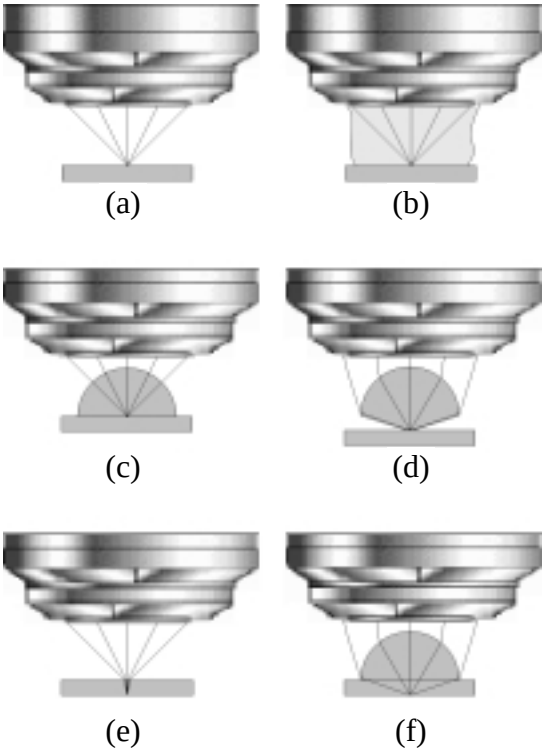

Fig. 1 Microscopy techniques.

In subsurface microscopy immersion techniques cannot increase *n*, however, θ can be increased in many circumstances. In standard subsurface microscopy of planar samples, despite having larger *n* in the object space, the *NA* remains unchanged due to refraction at the planar boundary, as illustrated in Fig. 1(e). This refraction also imparts spherical aberration that increases monotonically with *NA*, which without correction reduces the resolution. Though this is the common method for subsurface imaging of planar samples, even with an objective corrected for imaging at a certain depth, the maximum *NA* will still be less than 1. The Numerical Aperture Increasing Lens (NAIL) subsurface microscopy technique shown in Fig. 1(f) and described below can significantly increase the *NA* to *n* without introducing spherical aberration and thus improve the resolution.

The Numerical Aperture Increasing Lens (NAIL) is placed on the planar surface of a sample as illustrated in Fig. 2. Ideally the NAIL is made of the same material as the sample, both polished allowing an intimate contact to avoid reflections at the planar interface. We consider a NAIL of material with *n* matching that of the sample in order to minimize spherical aberration at the planar interface. A NAIL of material with *n* close to that of the sample behaves and can be analyzed similarly. The convex surface of the NAIL is spherical with a radius of curvature of *R*. The vertical thickness of the NAIL is *D*, which may be greater or less than *R*. Light is collected through the sample and NAIL from an object space in the sample at a vertical depth of *X*. To increase the *NA* without

introducing spherical aberration, *D* will selected to be *R×(1+1/n)–X*. By doing so the object space coincides with the aplanatic points of the NAIL's spherical surface, which satisfies the sine-condition yielding spherical aberration free or stigmatic imaging[6]. This is similar to the solid immersion lens[3,4] technique where the total lens depth is *R×(1+1/n)*. We will develop the location of this spherical aberration free area in terms of the NAIL parameters below.

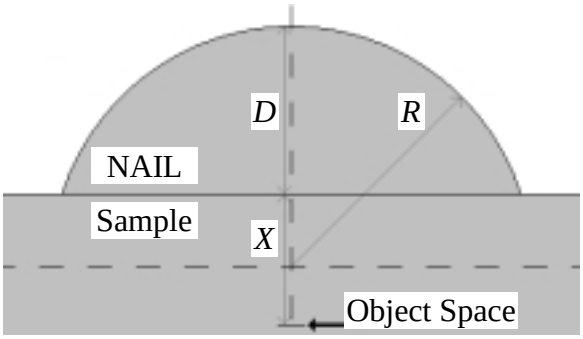

Fig. 2 Schematic of NAIL and sample parameters.

Ray optics will be used to demonstrate the NAIL method, because this is a far-field imaging technique. The spherical symmetry about the geometrical center of the spherical surface of the NAIL permits us to find radial solutions and generalize them. The limits of the generalization will be detailed afterwards. Fig. 3 defines the variables and coordinates to be used. We will consider the NAIL and sample to be a single piece of material of index *n*. The standard collection focus would be at a point (a) if nothing were in the optical path. The altered collection focus will be at a point (b) with the NAIL and sample in the optical path. Both of these points intersect the vertical collection ray (c) passing through the geometrical center. The collection ray path (d) is altered by Snell's law:

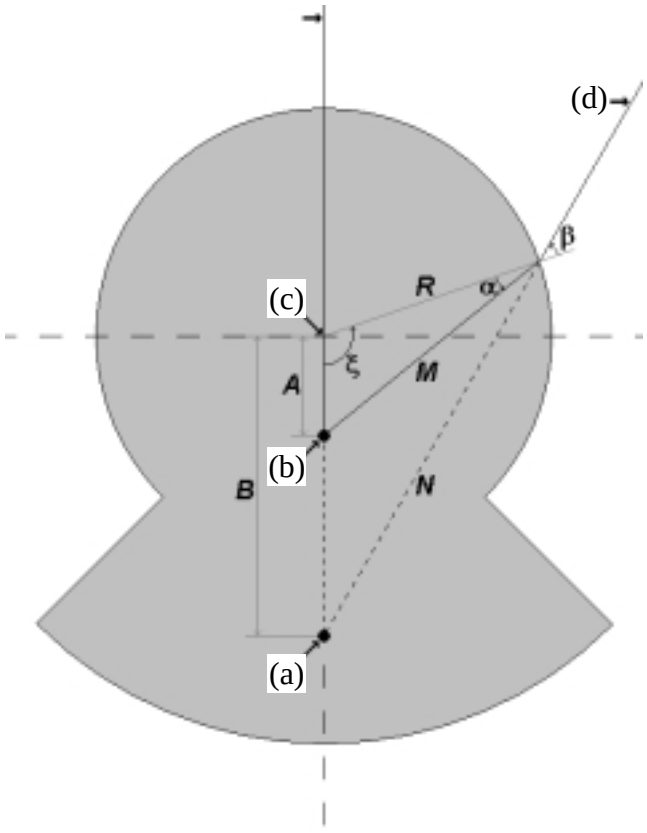

Fig. 3 Combined NAIL-sample representation.

$$\sin\beta = n \cdot \sin\alpha .$$

The Law of Sines yields:

$$\frac{\sin\alpha}{A} = \frac{\sin\xi}{M} \qquad \frac{\sin\beta}{B} = \frac{\sin\xi}{N}$$

Combining equations:

$$\frac{\sin\beta}{\sin\alpha}=\frac{B\cdot M}{A\cdot N}=n \qquad\qquad B^2\cdot M^2=n^2\cdot A^2\cdot N^2$$

The Law of Cosines yields:

$$M^2=R^2+A^2-2\cdot R\cdot A\cdot\cos\xi \qquad\qquad N^2=R^2+B^2-2\cdot R\cdot B\cdot\cos\xi$$

Combining equations we obtain an equation dependent only upon *n*, *R*, *A*, *B*, and ξ:

$$B^2\cdot\left(R^2+A^2-2\cdot R\cdot A\cdot\cos\xi\right)=n^2\cdot A^2\cdot\left(R^2+B^2-2\cdot R\cdot B\cdot\cos\xi\right)$$

To simplify we will switch to collection focus radial distance parameters that are normalized to *R*:

$$a=\frac{A}{R} \qquad\qquad b=\frac{B}{R}$$

$$b^2\cdot\left(1+a^2-2\cdot a\cdot\cos\xi\right)=a^2\cdot\left(1+b^2-2\cdot b\cdot\cos\xi\right)$$

Regrouping the terms we obtain:

$$\left(\frac{1}{a}+1\right)^2-n^2\cdot\left(\frac{1}{b}+1\right)^2=2\cdot(1+\cos\xi)\cdot\left(\frac{1}{a}-\frac{n^2}{b}\right) \qquad (1)$$

There are two solutions that are independent of ξ that therefore exhibit no spherical aberration:

$$\begin{pmatrix}A\\B\end{pmatrix}=R\cdot\begin{pmatrix}a\\b\end{pmatrix}=\begin{pmatrix}0\\0\end{pmatrix} \qquad\qquad \begin{pmatrix}A\\B\end{pmatrix}=R\cdot\begin{pmatrix}a\\b\end{pmatrix}=R\cdot\begin{pmatrix}\frac{1}{n}\\n\end{pmatrix}$$

A is the altered collection focus radial position and *B* is the standard collection focus radial position. The spherical symmetry about the geometrical center of the spherical surface permits us to generalize these radial solutions by rotation in the spherical coordinates θ,ϕ as shown in Fig. 4. The first solution has both the standard and altered collection focus at the geometrical center of the spherical surface of the lens. The SIL utilizes this first solution for imaging[2].

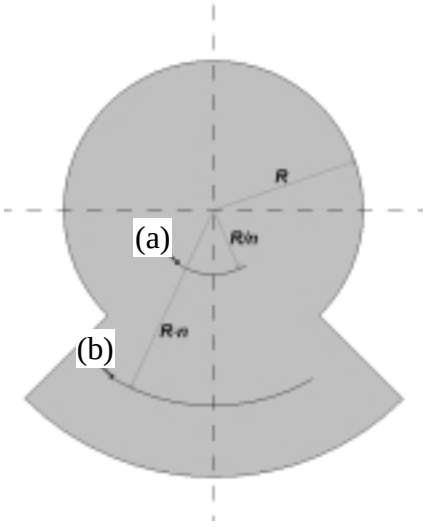

Fig. 4 Solutions of Equation 1.

The second solution provides an altered collection focus spherical surface (a) and a standard collection focus spherical surface (b). This altered collection focus spherical surface (a) will be referred to as the super-SIL[3,4] and NAIL spherical aberration free surface. Tolerance issues and volume imaging require that we also examine the properties of imaging outside of the spherical aberration free surface.

Parameters such as NAIL collection focus position, magnification, and spherical aberration will be derived for the area outside of the NAIL spherical aberration free surface. The right side of Equation 1, is the spherical aberration term and represents the error in the collection focus position. Spherical aberration is minimized for paraxial rays, rays that make small angles with respect to the optical axis. In this layout rays with $\xi \approx \pi$ are paraxial, and the spherical aberration term goes to zero with the paraxial approximation $(1+\cos\xi) \approx 0$. All of the variables on the left side of Equation 1 are positive quantities so the resulting paraxial solution is:

$$\left(\frac{1}{a_p}+1\right) = n \cdot \left(\frac{1}{b}+1\right) \qquad (2)$$

This paraxial solution a_p represents the NAIL collection focus position for paraxial rays having a standard collection focus at *b*. The magnification of the NAIL is divided into two components the tangential magnification and radial magnification. Due to the spherical symmetry the tangential magnification within the paraxial approximation is:

$$M_t = \frac{2 \cdot \pi \cdot d\theta \cdot d\phi \cdot B}{2 \cdot \pi \cdot d\theta \cdot d\phi \cdot A_p} = \frac{b}{a_p} = \frac{n}{1-(n-1) \cdot a_p}$$

In the vicinity outside of the spherical aberration free surface the tangential magnification is about $M_t = n^2$. The radial magnification within the paraxial approximation is:

$$M_r = \frac{dB}{dA_p} = \frac{n}{\left(1-(n-1) \cdot a_p\right)^2}$$

In the vicinity outside of the spherical aberration free surface the radial magnification is about $M_r = n^3$. So far in this section we have neglected the effects of spherical aberration, because to quantify it we would have to solve Equation 1. Since we are interested in the vicinity outside of the NAIL spherical aberration free surface we will use variables that reduce to a simpler form when this approximation is taken:

$$a = \frac{1}{n-n^2 \cdot (\delta+\varepsilon)} \qquad a_p = \frac{1}{n-n^2 \cdot \delta}$$

From Equation 2 we obtain:

$$b = \frac{n}{1 - n^2 \cdot \delta}$$

Substitution into Equation 1 yields:

$$\varepsilon = \frac{-(n-1)}{\frac{n+1-n^2 \cdot \left(\delta - \frac{\varepsilon}{2}\right)}{1+\cos\xi} - 1} \cdot \delta$$

If we consider δ, ε << 1, which represents the vicinity outside of the NAIL spherical aberration free surface then the following approximations follow:

$$a = \frac{1}{n} + \delta + \varepsilon \qquad a_p = \frac{1}{n} + \delta \qquad \varepsilon = \frac{-(n-1)}{\frac{n+1}{1+\cos\xi} - 1} \cdot \delta$$

We choose δ as the radial distance from the spherical aberration free surface, and ε as the resulting longitudinal spherical aberration, because there is no spherical aberration in the paraxial solution a_p. The last equation shows that ε increases the farther we move away from the paraxial approximation. We also see that ε is proportional to δ, so near the NAIL spherical aberration free surface, for small δ, we have a relatively spherical aberration free proximity. This NAIL spherical aberration free surface and relatively spherical aberration free proximity constitute a low spherical aberration shell.

So far we have used spherical symmetry to simplify our analysis, however the layout of the sample and NAIL will determine limits on the collection angular range. There are two limits on the collection area as illustrated in Fig. 5. The first limit (a) is the edge of the NAIL, the intersection of the spherical surface and planar boundary. This limit exists because light at angles beyond this limit does not encounter the spherical surface. When the NAIL collection focus (b) is on the spherical aberration free surface, the second limit (c) exists because light beyond the critical angle encounters total internal reflection. NAIL imaging at off-axis distances much less than *R/n* minimizes this limit. These two limits combine to yield collection angular range (d). Collection outside of this range will only introduce additional noise, as

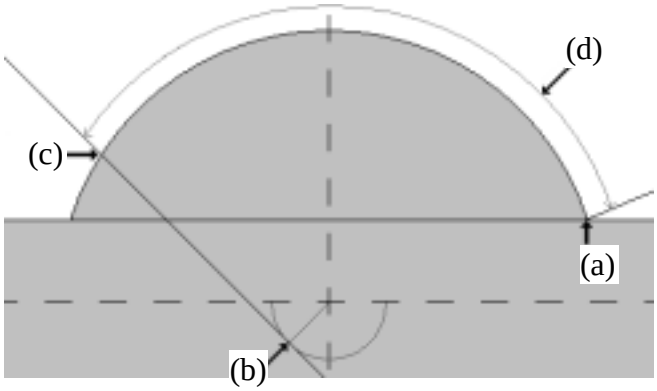

Fig. 5 Limits on collection angular range.

stray light from other points. Another advantage of NAIL imaging at off-axis distances much less than *R/n* is the low spherical aberration shell can be approximated as a planar sheet (a) as shown in Fig. 6. Again the vertical distance below the sample surface to the planar sheet is *X*. The resulting NAIL thickness *D* according to the NAIL solution to Equation 1 will be:

$$D = R\left(1+\frac{1}{n}\right) - X$$

Given the sample depth to be imaged *X*, suitable NAIL parameters must be determined to optimize collection. First we will derive the relationship that demonstrates the factor of n^2 improvement in *NA* and corresponding resolution. The *NA* of standard collection is $NA_s = \sin\theta_s$, and the *NA* with the NAIL on the sample is $NA_n = n \cdot \sin\theta_n$. According to Snell's law and the layout:

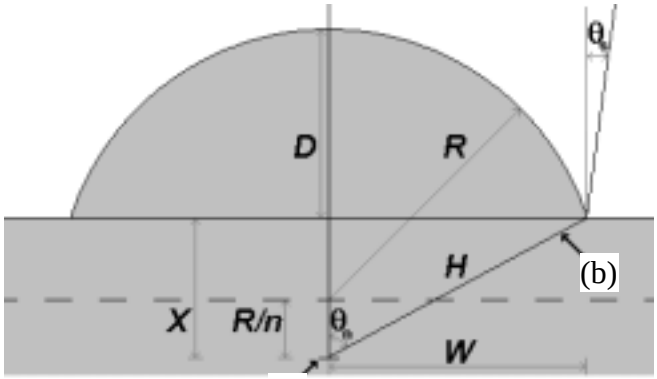

(a)

Fig. 6 Evaluation of NAIL limitation on *NA*.

$$\sin\theta_n = n \cdot \sin\theta_s$$

These equations combine to form the relationship:

$$NA_n = n^2 \cdot NA_s$$

This demonstrates the factor of n^2 improvement in *NA* and corresponding resolution. The collection angular range discussed above limits this improvement. Next we will develop the maximum value of the *NA* in terms of the NAIL parameters. Fig. 6 defines the variables and shows the highest angle collection ray (b). The layout yields:

$$NA_{n-\max} = n \cdot \sin\theta_{n-\max} = n \cdot \frac{W}{H} \qquad W^2 = R^2 - \left(X - \frac{R}{n}\right)^2 \qquad H^2 = W^2 + X^2$$

Therefore the maximum *NA* of the collected light is

$$NA_{n-\max} = n \cdot \sqrt{1 - \frac{\left(\frac{X}{R}\right)^2}{1 - \frac{1}{n^2} + \frac{2}{n} \cdot \left(\frac{X}{R}\right)}}$$

The maximum *NA* is slightly smaller for imaging at off-axis distances much less than *R/n*. The NAIL creates an n^2 increase in the collection *NA* up to this maximum *NA*. For a given sample depth *X*, the maximum *NA* increases monotonically with increasing *R*.

The appropriate solutions to the NAIL parameters must be determined according to the governing equations of the NAIL parameters developed so far and the layout limitations of the system into which the NAIL will be integrated.

Larger values of *R* should be used to flatten the low spherical aberration shell and maximize *NA*. This is often limited by the layout limitations of the system into which it is integrated such as the working distance of the microscope objective. An appropriate *R* should be chosen such that $R(1+1/n)$ is less than the working distance and accommodates the other layout limitations of the system into which it is integrated. A set of NAILs could be fabricated each with the same *R* and a set of different values of *D*. for a given system so imaging could be conducted at a range of sample depths *X*. Given a maximum allowable ε the separation of these values of *D* should be less than δ to eliminate the effects of spherical aberration. If many values of *D* were available, then imaging could be performed at any depth in a material without introducing spherical aberration. If the system requires only a small *NA* then the NAIL can be thin and small, however if a large *NA* is needed then a thicker NAIL must be used. In the next section we will analyze the limitations of collection and a NAIL microscope design that optimizes collection.

In many applications it is important to collect light from as much of the NAIL's area as possible to maximize *NA* and gain the best resolution. However, collecting light outside the NAIL introduces additional noise as stray light from other points. Limiting the collection *NA* of a detector is practical technique in imaging, because it minimizes noise collection while maximizing signal collection. The detector design or a confocal arrangement can accomplish this. The following NAIL microscope combined with a collection *NA* limited detector optimizes signal collection from the NAIL.

The right side of Fig. 7 is an enlargement of a sample and NAIL. The rays from a standard collection focus (a) at an off axis distance ρ much less than $R \cdot n$ have an average angular

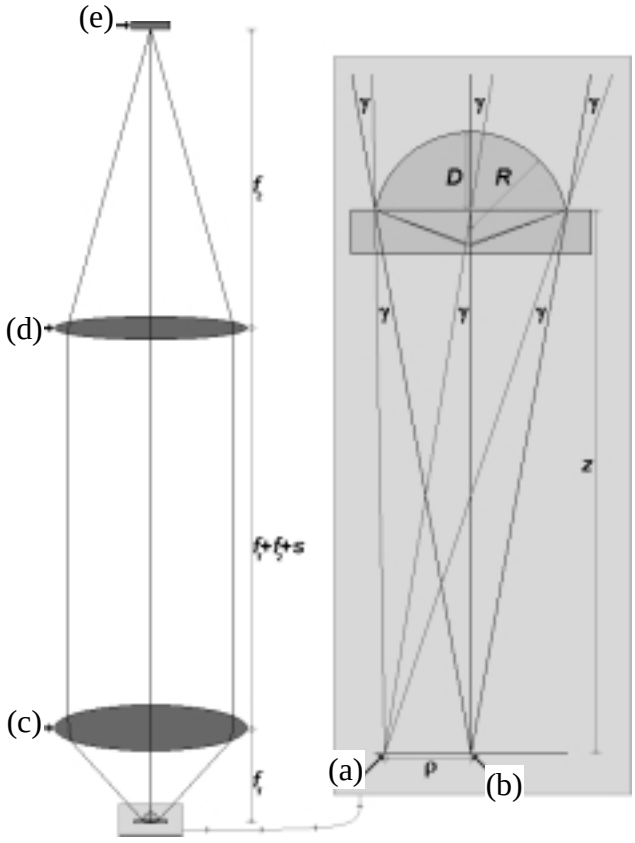

Fig. 7 NAIL microscope configuration.

displacement γ relative to the rays from on axis standard collection focus (b). The layout and parameters of this NAIL yields:

$$z = R \cdot (n+1) - D \qquad \gamma \approx \frac{-\rho}{z}$$

Combining equations:

$$\gamma \approx \frac{-\rho}{R \cdot (n+1) - D}$$

Notice that the angular displacement γ is proportional to the distance ρ. The NAIL microscope eliminates this effect so rays from any off axis point do not have an angular displacement at the *NA* limited detector. On the left side of Fig. 7 is the NAIL microscope configuration and parameters. The NAIL, objective lens (c)**,** tube lens (d), and collection *NA* limited detector (e) are all aligned along the optical axis. The objective lens has a focal length f_1 and tube lens has a focal length f_2. They are considered to be ideal lenses for calculations by the lens law, but their real counterparts will of course introduce nominal aberrations. The collection angle is usually small enough that the paraxial approximation can be taken, and a ray-transfer matrix for the microscope can be established. The following relationships result from this arrangement:

$$\begin{bmatrix} \rho_2 \\ \theta_2 \end{bmatrix} = \begin{bmatrix} -\frac{f_2}{f_1} & 0 \\ \frac{s}{f_1 \cdot f_2} & -\frac{f_1}{f_2} \end{bmatrix} \begin{bmatrix} \rho_1 \\ \theta_1 \end{bmatrix} \qquad \theta_2 = \left(\frac{s}{f_1 \cdot f_2} \right) \cdot \rho_1 + \left(-\frac{f_1}{f_2} \right) \cdot \theta_1$$

In order to collect the full amount of light while filling the detector *NA*, the two effects can counteract each other and cancel given an appropriate value of s.

$$\left(\frac{s}{f_1 \cdot f_2} \right) \cdot Y_1 + \left(-\frac{f_1}{f_2} \right) \cdot (-\alpha) = 0 \qquad \left(\frac{s}{f_1 \cdot f_2} \right) \cdot Y_1 + \left(-\frac{f_1}{f_2} \right) \cdot \left(-\frac{Y_1}{R\left(n + \frac{1}{n} \right)} \right) = 0$$

$$s = \frac{-f_1^{\,2}}{R\left(n + \frac{1}{n} \right)}$$

In summary the NAIL microscope will collect light from only the full NAIL area thereby maximizing the *NA* and the resolution while collecting as much signal as possible without outside noise.

Current Si integrated circuit (IC) technology includes many opaque metal layers and structures above semiconductor devices, thereby hindering topside inspection of these buried devices in their final state. Therefore, inspection through the backside or substrate of the Si IC is often preferred[7]. However, optical absorption in Si limits inspection through the substrate to a λ_0 greater than 1 μm, yielding a theoretical resolution limit for standard subsurface microscopy of approximately 0.5 μm. Typical resolution values for commercial systems are about 1 μm. Meanwhile, modern Si IC technology has reached process size scales of 0.13 μm, clearly beyond the capability of standard subsurface microscopy. Using the NAIL microscopy technique the theoretical resolution limit is improved to 0.14 μm. We experimentally demonstrate an estimated resolution of better than 0.2 μm, to the best of our knowledge a spatial resolution record for backside inspection of Si ICs.

A Si IC fabricated by a 0.25 μm process is inspected using our NAIL microscope. A Si NAIL is placed on the polished backside of the Si substrate as illustrated in Fig. 8. The specific NAIL we used has an *R* of 1.6 μm and a *D* of 1.5 μm, optimized for an *X* of 500 μm, the polished substrate thickness. The NAIL infinity corrected confocal scanning optical microscope configuration is illustrated Fig. 9. The 0.3-NA microscope objective lens achieves the highest *NA* of 3.4 for this NAIL. A 25 mm pinhole is placed in the image plane in a confocal arrangement and the NAIL and sample are scanned to form an image. A 1.05 μm laser diode provides bottom illumination to the sample at which wavelength a cooled germanium detector offers a high detectivity. At this λ_0 the increase in *NA* is a factor of 13, with an upper limit on *NA* of 3.4 for this NAIL, and consequently the resolution limit is improved to 0.15 μm. The precision of the scan is relaxed by a factor of 13, so a 13 μm mechanical movement of the NAIL and sample results in a 1 μm focal point movement in the object space. Our instrument mechanically scanned 200 μm by steps of 1 μm to create a 15 μm image with pixels of 0.08 μm.

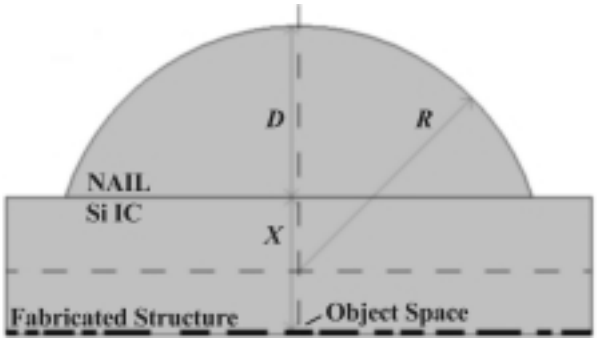

Fig. 8 Si NAIL placed on Si IC.

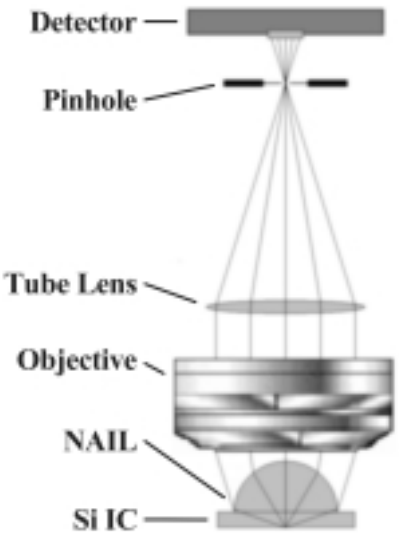

Fig. 9 NAIL microscope.

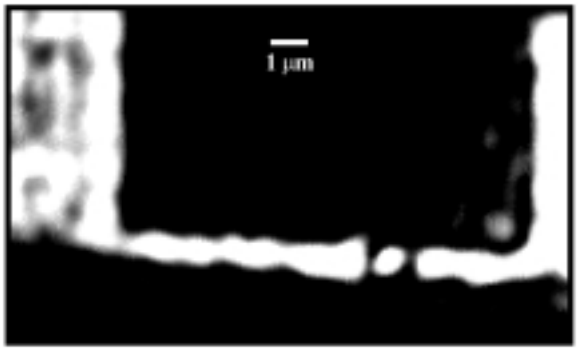

Fig. 10 Large area (15 μm × 9 μm) image

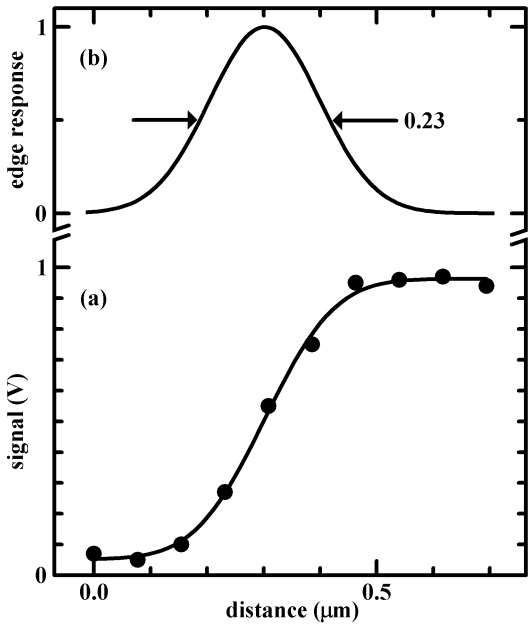

Fig. 11 Horizontal line cut of an edge (a) detector signal plotted by distance in the horizontal direction (b) fitted edge response.

A large area scanned image of 15 μm × 9 μm is shown in Fig. 10. The grayscale in this image represents the detector signal; transmission is blocked where it is dark.

By measuring an edge response we can evaluate the resolution of the microscope. Figure 11(a) is a horizontal line cut along the edge in the upper right side of this image, showing the detector signal plotted by distance in the horizontal direction. Fitting this edge we obtain the edge response shown in the Fig. 11(b), displaying a full-width-at-half-maximum (FWHM) of 0.23 μm. The measured FWHM represents a convolution of the NAIL microscope response and the physical structure. Based on the expected physical edge width for the 0.25 μm fabrication process, we estimate the NAIL microscope resolution to be better than 0.2 μm.

In conclusion, the NAIL subsurface microscopy technique we describe significantly increases the NA without introducing spherical aberration and consequently improves the resolution beyond the limit of standard subsurface microscopy. Using the NAIL technique in the near infrared inspection of Si ICs the theoretical resolution limit is improved from 0.5 μm to 0.14 μm, experimentally by realizing 3.4-NA we demonstrate an estimated resolution of better than 0.2 μm. In addition to first implementation there are a variety of other subsurface microscopy applications for the NAIL technique including visible, biological, and thermal imaging as well as other semiconductor applications.

The authors would like to acknowledge JDS Uniphase for providing the laser diode, and the DARPA HERETIC Program for supporting this project.

[1] C. M. Sparrow, ApJ, 44, 76 (1916).
[2] S. M. Mansfield and G. S. Kino, Appl. Phys. Lett. 57, 2615 (1990).
[3] B. D. Terris, H. J. Mamin, D. Rugar, W. R. Studenmund, and G. S. Kino, Appl. Phys. Lett. 65, 388 (1994).
[4] K. Karrai, X. Lorenz, and L. Novotny, Appl. Phys. Lett. 77, 3459 (2000).
[5] Q. Wu, G. D. Feke, and R. D. Grober, Appl. Phys. Lett. 75, 4064 (1999).
[6] M. Born and E. Wolf, *Principles of optics*, **7**th edition (Cambridge University Press, New York, 1999), pp. 465 and 159.
[7] For example the semiconductor failure analysis instruments of Hamamatsu Corporation, 360 Foothill Road, Bridgewater, NJ 08807